

WBANs-Spa: An Energy Efficient Relay Algorithm for Wireless Capsule Endoscopy

Dan Liu^{1,2}, Yishuang Geng², Guanxiong Liu², Mingda Zhou² and Kaveh Pahlavan²

¹ College of Information Engineering, Dalian Ocean University (DLOU), Dalian, Liaoning, China, 116020

² Center for Wireless Information Network Studies (CWINS), Worcester Polytechnic Institute (WPI), Worcester, MA, 01609
Email: liudan@dloou.edu.cn and {ygeng, gliu2, mzhou2 and kaveh}@wpi.edu

Abstract—Wireless Body Area Networks (WBANs) are specific purpose sensor networks designed to operate autonomously to connect various medical sensors, located inside and outside of a human body. WCE quickly becomes one of the most popular WBANs applications. Due to finite energy budget of sensor nodes, transmission power should be as low as possible in order to increase the life time of WBANs. To this end, we addressed a relay network model from in-body Wireless Capsule Endoscopy (WCE), to on-body relay nodes, and finally to external Access Point (AP) for the energy-efficient of WBANs in heterogeneous environment for realistic medical applications. Also, we proposed WBANs-Shortest Path Algorithm (WBANs-Spa) of relay network to reduce total network power consumption using empirical pathloss model, which could find the optimal multi-hop path based on the network model. Simulation results showed our design was effective for minimizing total network energy consumption in relay network for WBANs, and the effect of on-body relay nodes and external AP deployment was provided.

I. INTRODUCTION

Wireless Body Area Networks (WBANs) are specific purpose sensor networks designed to operate autonomously to connect medical sensors, located inside and outside of a human body. The latest standardization of WBANs, IEEE 802.15.6, aims to provide an international standard for low power, short range and extremely reliable wireless communication [1]. Due to finite energy budget of WBANs, transmission power should be as low as possible in order to increase sensors' life time. In previous work, some sensors, which are called relay nodes or relays, are added to the WBANs to collect and send the information to the receiver through multi-hop wireless paths. These relays play an important role in reducing the transmission power of biosensors and energy consumption of networks [2]. As a result, relay nodes (embedded within the clothes or disposable overall) can give WBANs devices a longer life time [3], further decrease the power consumption of biosensor in the body [4].

Wireless Capsule Endoscopy (WCE) is one of the most popular WBANs application for diagnostic of intestinal diseases [5][6]. It is a pill-shape device equipped with at least one camera, taking dozens of thousands of images while going through patients gastrointestinal (GI) tract. Due to anatomic characteristics of human body and the shortcomings of traditional inspection equipment, it was always challenging for physicians to identify abnormalities inside the GI tract until the birth of WCE. Similar to other WBANs application, the transmission power of WCE is strictly limited to avoid the undesired radiation overdoses. Since the WCE power budget is also limited, an energy efficient solution is highly necessary. Presently, most of ongoing research is focusing on the development of the transmitter hardware design to reduce the capsules power consumption [7][8]. But, few of them have

taken the complete relay network model from in-body (WCE) to on-body (relay), and finally to external Access Point (AP) into consideration.

In this paper, we propose a novel WBANs-Spa relay algorithm to reduce the power consumption of the relay network for WBANs in heterogeneous environment with pathloss model based on such network model. We first design a belt equipped with different numbers of relays on the body. Then a WCE is allocated inside large intestine and small intestine to form the path of WCE and an external AP outside human body is added as the receiver. Then, we designed a novel energy efficient WBANs-Spa algorithm based on empirical wireless propagation channel models and classic shortest path algorithm for the relay network, finding the optimal multi-hop path with minimum overall power consumption. Finally, a set of Monte Carlo simulations were carried out to evaluate the performance of our design. Since the major energy cost for the relay network is to transmit information in a lossy medium, we minimized the energy consumption in the perspective of passloss.

The rest of this paper is organized as follows: We begin in Section II by introducing the system model. After that, we make our novel design of energy-efficient relay network for WBANs in section III. In section IV, we provide simulation results which highlight the performance using the WBANs-Spa. Finally, we conclude the paper in section V.

II. SYSTEM MODEL

A. WBANs Communication System Model

The WBANs communication system employed in this study can be abstracted into three critical components, namely,

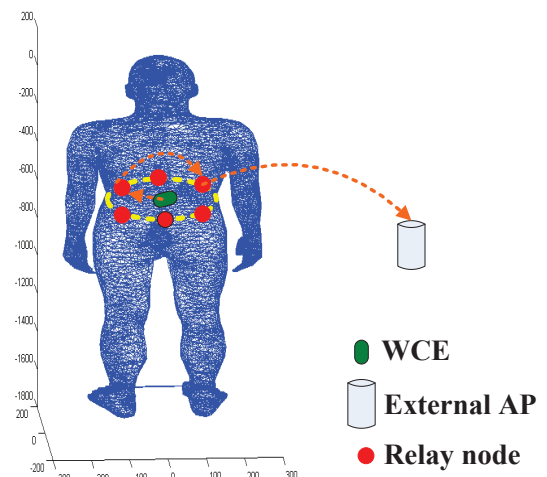


Fig. 1: A typical communication system model with 6 relay nodes for WBANs.

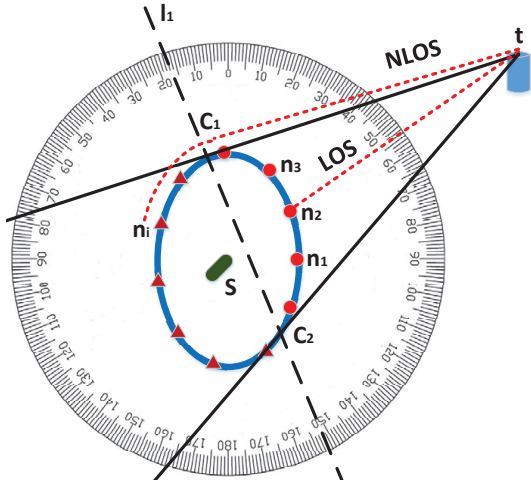


Fig. 2: Ellipsoid section of human waist with LOS and NLOS cases.

source node s , destination node t and a relay network with totally N nodes as $R = \{n_1, n_2, \dots, n_N\}$. Clearly, when applying such abstraction to the WCE application, s is the capsule pill that emits RF signal from inside of human GI tract, t is the external AP that is designed to collect the transmitted bits and n_i is the i th on-body relay node. All relay nodes are evenly distributed on a specific belt with the first relay node n_1 always fixed in the middle of the front side of human body. Note that we approximate the human waist with an ellipse. A typical system with six relay nodes has been provided in Fig. 1, where the belt is assumed to be at the average height of small and large intestine.

Three types of connections can be setup with the communication system as (1) In-body links $s \rightarrow n_i$, the link from capsule pill to the i th on-body relay node; (2) On-body links $n_i \rightarrow n_j$, the on-body link from i th relay node to j th relay node; (3) Off-body links $n_j \rightarrow t$, the link from j th on-body relay node to the external AP. The in-body links operate on Medical Implant Communication Service (MICS) band, which is from 402 to 405MHz. Such narrow band is designed to guarantee enough coverage of the implantable devices. The RF waves travel in the pattern of creeping wave on the surface of human body and the on-body links are designed to be at Ultra-Wide Band (UWB) band to save power and guarantee acceptable data rate. Off-body links also operate on UWB band but they are more complicated since it is possible to have the direct line-of-sight blocked by part of the human body. To deal with that issue, we partition the off-body links into line-of-sight (LOS) and non-line-of-sight (NLOS) cases.

As is stated in [9], when NLOS occurs, the RF signal cannot penetrate the human body due to the severe absorption. Instead, it first goes as creeping wave and then gets scattered at the cut-point when LOS is available. To effectively display the

TABLE I: Parameters for IEEE 802.15.6 in-body radio propagation channel, from implant to body surface.

Implant to Body Surface	$L_p(d_s)$ (dB)	α_s	σ_s (dB)
Deep tissue	47.14	4.26	7.85
Near surface	49.81	4.22	6.81

LOS and NLOS cases, we plot the ellipsoid section of human waist in Fig. 2. As can be seen from the figure, two tangent lines of the ellipse can be found from t with cut-point c_1 and c_2 . By connecting the two cut-points, line l_1 can be found to separate the entire 2D coordinate space. We define n_i in LOS case if n_i and t are at the same side of l_1 and n_i in NLOS case if they are at different side of l_1 . In Fig. 2, we label LOS nodes with red circle and NLOS nodes with red triangle for illustration.

It is easy to observe when NLOS occurs, there are two NLOS paths going either clockwise or counter-clockwise. Since the RF signals suffer from severe propagation loss and longer delay when it creeps on the surface of human body, the shorter path always dominates the wireless communication. We define c_m as the closest cut-point to relay node n_i that provides shortest NLOS path. In Fig. 2, we have $c_m = c_1$ as a brief example. Frii's equation and references [1][9] shows that the coverage of all employed nodes are way beyond the scale of our communication system, we assume that fully connection can be obtained for all three types of connections, that is, for $s \rightarrow n_i$, $n_i \rightarrow n_j$ and $n_j \rightarrow t$, we have $i \neq j$ and $i, j \in [1, N]$. With the above mentioned communication model, the images of inside small and large intestine can be transmitted to the external AP through the relay network.

B. WBANs Radio Propagation Channel Model

As is mentioned in the previous subsection, three types of wireless channel have been included in the WBAN communication system model, in this section, we provide the detailed formulation for the pathloss calculation. Since the radio signals are initially emitted from the capsule endoscopy, we start our discussion from the statistic radio propagation channel from implant to relay nodes at MICS band. According to IEEE 802.15.6 standard channel model [1], the in-body pathloss can be given as

$$L_p(d_{s,i}) = L_p(d_s) + 10\alpha_s \log_{10} \frac{d_{s,i}}{d_s} + \sigma_s, \quad i \in [1, N] \quad (1)$$

where $L_p(d_{s,i})$ is the in-body propagation pathloss, $d_{s,i}$ denotes the actual distance between the capsule endoscopy and the i th on-body relay node, N is the total number of nodes in the system except for the capsule and external AP, $L_p(d_s)$ is the pathloss at reference distance d_s , which is 50mm in this work. α_s denotes the distance-power gradient and σ_s shows the effect of shadow fading, which is created by the slight movement of human organs. Note that the implant to body surface channel has two sets of different parameters for deep tissue scenario ($d_{s,i} \geq 10mm$) and near surface scenario ($d_{s,i} < 10mm$), we list all the parameters in Table I.

Regarding the wireless channel between a pair of on-body relay nodes, the pathloss is modeled with respect to the on-body curly distance between the nodes [1]. However, since an angle based deployment has been employed in this work, we adopt the equivalent angle based pathloss model as [10]

$$L_p(\theta_{i,j}) = L_p(\theta_0) + \gamma(\theta_{i,j} - \theta_0), \quad i \neq j \text{ and } i, j \in [1, N] \quad (2)$$

where $L_p(\theta_{i,j})$ is the on-body propagation pathloss, $\theta_{i,j}$ denotes to the actual central angle between the i th and j th on-body relay node, $L_p(\theta_0) = 44.25dB$ is the pathloss at

reference central angle θ_0 , which is 0.3115rad in this work. $\gamma = 16\text{dB/rad}$ denotes to the angle-power gradient.

The wireless channel from on-body relay node to external AP can be partitioned into LOS scenario and NLOS scenario. In LOS scenario, the IEEE 802.15.3a model can be directly applied as

$$L_p(d_{j,t}) = L_p(d_t) + 10\alpha_t \log_{10} \frac{d_{j,t}}{d_t} + \sigma_t, \quad j \in [1, N] \quad (3)$$

where $L_p(d_{j,t})$ is the off-body propagation pathloss, $d_{j,t}$ denotes to the actual distance between the j th on-body relay node and the external AP, $L_p(d_t) = 47\text{dB}$ is the pathloss at reference distance d_t , which is 1m in this work. $\alpha_t = 1.7$ denotes to the distance-power gradient and $\sigma_t = 1.6\text{dB}$ shows the effect of shadow fading.

When NLOS occurs, the off-body pathloss is a combination of creeping wave from j th on-body relay node to the closest cut-point c_m , and LOS propagation from c_m to the external AP. Formulation of off-body pathloss in NLOS scenario can be provided using equation (2) and (3) as

$$L_p(d_{j,t}) = L_p(\theta_{j,c_m}) + L_p(d_{c_m,t}), \quad j \in [1, N] \quad (4)$$

Combining equation (3) and (4), the general form of off-body pathloss model can be given as

$$L_p(d_{j,N+2}) = \begin{cases} L_p(d_t) + 10\alpha_t \log_{10} \frac{d_{j,t}}{d_t} + \sigma_t, & \text{LOS} \\ L_p(\theta_{j,c_m}) + L_p(d_{c_m,t}), & \text{NLOS} \end{cases}, \quad j \in [1, N] \quad (5)$$

With the channel models in equation (1), (2) and (5), the pathloss of each link in the system model can be therefore calculated.

III. ALGORITHM DESIGN

With the system model and channel models provided in the previous sections, the remaining work would be designing an algorithm that can minimize the overall pathloss from WCE to external AP. It is intuitive that such minimization problem can be solved by existing infrastructure in graph theory. In this section, we convert the relay network into a graph and find the minimum overall network pathloss by a single-source shortest path algorithm. The proposed algorithm is named as WBANs-Spa and it can be introduced in three steps as

•**Initialization.** As is shown in Fig. 3, we can represent the relay network by 2D matrix $G(i, j)$, $i, j \in [1, N+2]$ where each index i or j represents a node in the network and the value of $G(i, j)$ denotes the pathloss of link $(n_i \rightarrow n_j)$. Note that we increase the dimension of i and j by 2 so that n_1

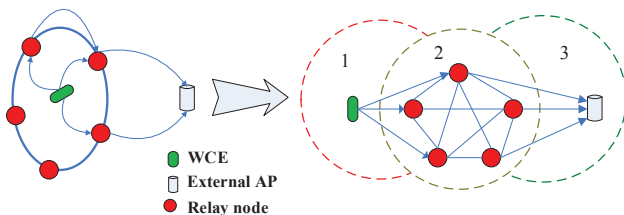


Fig. 3: Converting relay network into a graph.

Algorithm 1 . WBANs-Spa

```

1: //Initializing Graph  $G$  of pathloss
2: Initialize  $G \leftarrow \infty \times \text{ones}(N+2 \times N+2)$ 
3: for  $i$  from 1 to  $N$ 
4:    $G(i+1, N+2) \leftarrow L_p(d_{i, N+2})$  //Off-body pathloss
5:   for  $j$  from 1 to  $N$ 
6:     if  $i \neq j$ 
7:        $G(i+1, j+1) \leftarrow L_p(\theta_{i, j})$  //On-body pathloss
8:     else
9:        $G(1, j+1) \leftarrow L_p(d_{s, j})$  //In-body pathloss
10:       $G(i+1, j+1) \leftarrow \infty$  //On-body pathloss not exist
11:    end
12: //Keep track of minimum in/off-body pathloss for prune
13: Track  $m_1$  s.t.  $\forall G(1, j) \geq G(1, m_1)$ 
14: Track  $m_2$  s.t.  $\forall G(i, N+2) \geq G(m_2, N+2)$ 
15: end
16: end
17: //Pruning Graph  $G$  for optimization
18: for  $k$  from 1 to  $N$ 
19:   if  $G(1, k) > G(1, m_2)$ 
20:      $G(1, k) \leftarrow \infty$ 
21:   end
22:   if  $G(k, N+2) > G(m_1, N+2)$ 
23:      $G(k, N+2) \leftarrow \infty$ 
24:   end
25: end
26: //Running single source Dijkstra's Algorithm
27: Initialize-Single-Source( $G, s$ )
28:  $S \leftarrow \phi$ 
29:  $Q \leftarrow G$  (Converted to priority queue)
30: while  $Q \neq \phi$ 
31:    $i \leftarrow \text{Extract-Min}(Q)$ 
32:    $S \leftarrow S \cup i$ 
33:   foreach vertex  $j \in G.Adj[i]$ 
34:     Relax( $i, j, G(i, j)$ ) //Classic relaxation process
35:   end
36: end

```

denotes s , n_{N+2} denotes t . The first row $G(1, :)$ represents in-body pathloss, the last column $G(:, N+2)$ represents the off-body pathloss and the middle $N \times N$ submatrix is the on-body pathloss.

•**Pruning.** With a proper initialization, we realize that at least one in-body link and one on-body link has to be involved to fulfill the functionality of the communication system and the algorithm tries to by-pass severely attenuated in-body or off-body links by using the on-body relay network. For in-body links, there exists a link with minimum pathloss $(n_1 \rightarrow n_{m_1})$, **s.t.** $\forall (n_1 \rightarrow n_i) \geq (n_1 \rightarrow n_{m_1})$. Then any off-body link must satisfy that $(n_j \rightarrow n_{N+2}) \leq (n_{m_1} \rightarrow n_{N+2})$, otherwise, it will be by-passed by $(n_{m_1} \rightarrow n_{N+2})$ and no longer appears in the shortest path. Same thing happens for the off-body links. Given a link with minimum pathloss $(n_{m_2} \rightarrow n_{N+2})$, **s.t.** $\forall (n_j \rightarrow n_{N+2}) \geq (n_{m_2} \rightarrow n_{N+2})$. Then any in-body link must satisfy that $(n_1 \rightarrow n_i) \leq (n_1 \rightarrow n_{m_2})$. Using those criteria, we prune the graph to remove unnecessary in-body and on-body links to improve the algorithm efficiency.

•**Finding Shortest Path.** Finally, we run a classic single-source shortest path algorithm to find the path from n_1 to n_{N+2}

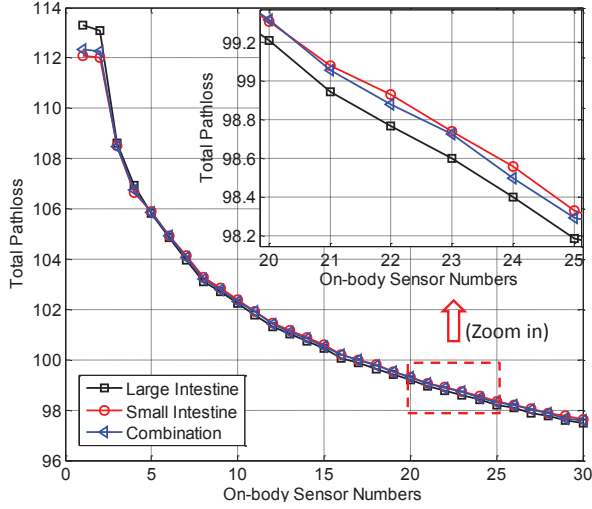


Fig. 4: Total power consumption for different number of relay nodes.

and record the overall pathloss for the shortest path. Note that the WCE travels inside human GI tract one step after another, the entire algorithm has to be constantly running for each step. The detailed algorithm has been depicted in *Algorithm 1*.

IV. SIMULATION RESULTS

The simulation setup is based on the application of WCE in small intestine and large intestine environments. Connectivity is assumed from WCE to relay, then to external AP. The pathloss parameters are determined by the length of each connection as mentioned in previous sections. In the following simulation, we added the number of relays one after another (ranging from 1 to 30) and assumed only one single capsule in each organ. The capsule is assumed to pass through small intestine and large intestine. According to the energy-efficient WBANs-Spa relay algorithm in section III, we calculated the corresponding pathloss for all the possible location points of WCE inside each organ (83 points for small intestine, 26 points for large intestine and 109 points for combination). 2000 trials of Monte Carlo simulation has been carried out to mitigate the effect of randomness from statistic channel models and each trial include the entire path of both small and large intestines. We average the pathloss from each Monte Carlo trial to collect the final results.

A. Effect of Relay Nodes Numbers

1) *Total Pathloss Along the Shortest Path*: In this subsection, we evaluate the impact of relay numbers on total network pathloss in large intestine, small intestine and combination separately. Total power consumption for different number of relay sensors is shown in Fig. 4. Notice that the total power consumption decreased gradually with the rising number of relay nodes by using the energy-efficient WBANs-Spa algorithm. When the number of relay nodes is 1 and 2, the power consumption does not decrease apparently. The main reason is that when the relay number is too small, there are no more optimal relays to select. So the difference of the shortest path is not obvious. With the number of relays being rising from 1 to 30, around 15.5dB total power can be saved. Notice that with a

relatively larger number of relays, the advantages of WBANs-Spa becomes less obvious. However, it can still save extra energy with more relays. It can be found from the zooming view that large intestine consume less power compared with small intestine, but the difference is only around 0.2dB and it is trivial.

2) *Pathloss of in-body Propagation*: In this subsection, we investigate the impact of relay numbers on in-body pathloss for different scenario of large intestine, small intestine and combination separately. In-body power consumption for different number of relay sensors is shown in Fig. 5. The result shows that the WCE power consumption decreased gradually with the rising number of relay nodes by using the energy-efficient relay networking. Notice that when the number of relays is 3 and 4, the separate pathloss is the same. That is due to the fact that the first relay is put on the middle front of human body. With the number of relays being rising, identical trend can be found with the previous subsection. It can be found from the

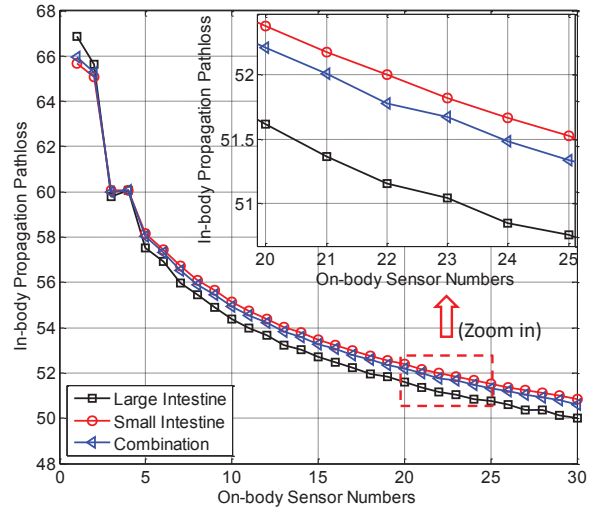


Fig. 5: In-body power consumption for different number of relay nodes.

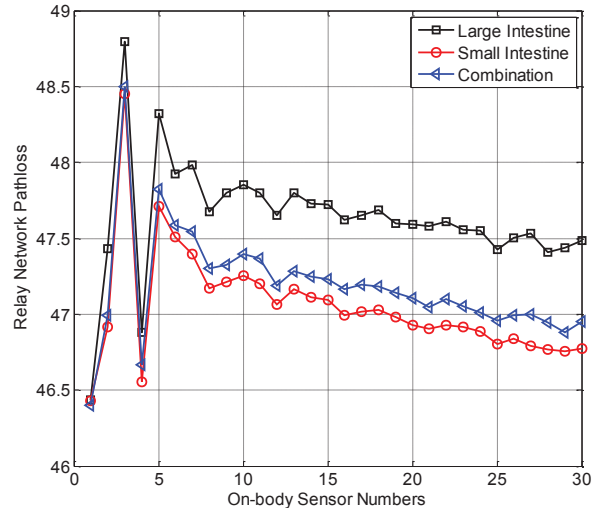


Fig. 6: Relay network power consumption for different number of relay nodes.

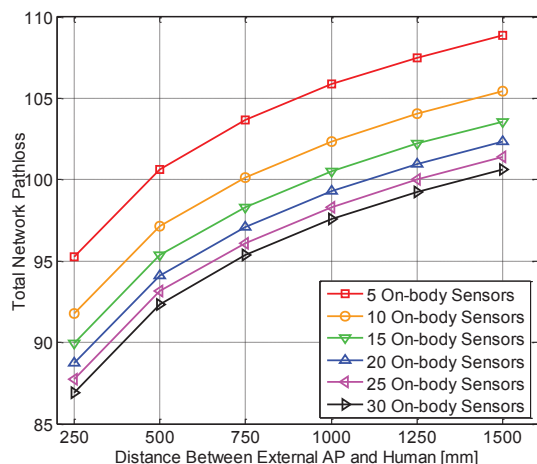


Fig. 7: Total power consumption for different distances between external AP and human body.

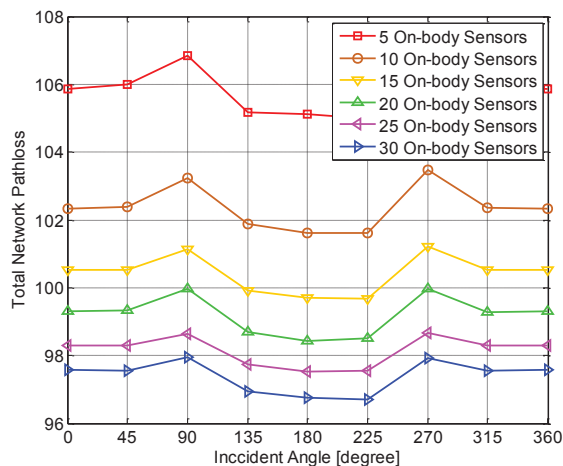


Fig. 8: Total power consumption for different incident angles. zooming view that WCE power consumption is the smallest in the large intestine, while the power consumption is the largest in the small intestine. The power consumption difference can be as large as 0.7dB.

3) *Pathloss of the Relay Network:* In this subsection, we evaluate the impact of relay numbers and total relay network pathloss for different scenario of large intestine, small intestine and combination. Relay network power consumption for different number of relay sensors is shown in Fig. 6. Notice that the relay network power consumption is the smallest in the small intestine, while the power consumption is the largest in the large intestine with the number of relays being rising. With the first five relay, the pass loss changed lot. While the relay numbers rises, the pathloss decreased gradually.

B. Effect of Geometric Information

1) *Effect of Distance Between External AP and Human Body:* We investigate the impact of the total power consumption and distance between external AP and human in this subsection. The distance varies from 250mm to 1500mm by 250mm and the number of relay nodes increases by 5 each step. With the distance rising, the total network pathloss increases. While the pathloss is the smallest with the number of relay is 30, as shown in Fig 7.

2) *Effect of Incident Angle:* Lastly, we investigate the impact of the incident angle of external AP and total network pathloss. The AP is put on the angle increasing by 45 degree from 0 degree, while the 0 degree is the center of front body. Notice that when the angle of location for AP is 135,180 and 225, the total pathloss is the smallest. This means the back of body is the better location for AP. The results are presented in Fig. 8. While the degree of 270 is the worst AP location for the total pathloss.

V. CONCLUSION

In this paper we addressed a relay network model from in-body to on-body, then to external AP for WBANs in heterogeneous environment for realistic medical application, considering energy issues. We proposed a novel algorithm of relay network for minimum total power consumption with pathloss model based on the network model that shows (1) effect of on-body relay numbers and total network pathloss, (2) effect of relay numbers and total in-body pathloss, (3) effect of relay numbers and total relay network pathloss, as well as (4) effect of the external AP location and total network pathloss. Simulation results showed our WBANs-Spa was effective for minimizing the total power consumption for WBANs, and the effect of on-body relay nodes and external AP deployment was provided.

REFERENCES

- [1] IEEE standard for local and metropolitan area networks: Part 15.6: Wireless body area networks. IEEE submission, Feb. 2012.
- [2] Ehyae, Aida, Massoud Hashemi, and Pejman Khadivi. "Using relay network to increase life time in wireless body area sensor networks." In World of Wireless, Mobile and Multimedia Networks and Workshops, 2009. WoWMoM 2009. IEEE International Symposium on a, pp. 1-6. IEEE, 2009.
- [3] Bala, Renu. "An Energy Efficient Routing protocol in Wireless Body Area Networks." 2014.
- [4] Tauqir, Anum, Nadeem Javaid, S. Akram, A. Rao, and S. N. Mohammad. "Distance aware relaying energy-efficient: Dare to monitor patients in multi-hop body area sensor networks." In Broadband and Wireless Computing, Communication and Applications (BWCCA), 2013 Eighth International Conference on, pp. 206-213. IEEE, 2013.
- [5] Zhou, Mingda, Guanqun Bao, Yishuang Geng, Bader Alkandari, and Xi-aoxi Li. "Polyp detection and radius measurement in small intestine using video capsule endoscopy." In Biomedical Engineering and Informatics (BMEI), 2014 7th International Conference on, pp. 237-241. IEEE, 2014.
- [6] Bao, Guanqun, Liang Mi, Yishuang Geng, and Kaveh Pahlavan. "A Computer Vision based Speed Estimation Technique for Localizing the Wireless Capsule Endoscope inside Small Intestine." In 2014 IEEE 36th Annual International Conference of the IEEE Engineering in Medicine and Biology Society (EMBC).
- [7] Gao, Yuan, Yuanjin Zheng, Shengxi Diao, Wei-Da Toh, Chyuen-Wei Ang, Minkyu Je, and Chun-Huat Heng. "Low-power ultrawideband wireless telemetry transceiver for medical sensor applications." Biomedical Engineering, IEEE Transactions on 58, no. 3 (2011): 768-772.
- [8] Basar, Md Rubel, Mohd Fareq Bin Abd Malek, Mohd Iskandar Mohd Saleh, Mohd Shaharom Idris, Khairudi Mohd Juni, Azuwa Ali, Nur Adyani Mohd Affendi, and Nuriziani Hussin. "A novel, high-speed image transmitter for wireless capsule endoscopy." Progress In Electromagnetics Research 137 (2013): 129-147.
- [9] Geng, Yishuang, Yadong Wan, Jie He, and Kaveh Pahlavan. "An empirical channel model for the effect of human body on ray tracing." In Personal Indoor and Mobile Radio Communications (PIMRC), 2013 IEEE 24th International Symposium on, pp. 47-52. IEEE, 2013.
- [10] Chen, Jin, Yunxing Ye, and Kaveh Pahlavan. "UWB characteristics of creeping wave for RF localization around the human body." In Personal Indoor and Mobile Radio Communications (PIMRC), 2012 IEEE 23rd International Symposium on, pp. 1290-1294. IEEE, 2012.